Interannual variability of the coastal fog at Fray Jorge relict forests in semiarid Chile

René Garreaud,[1] Jonathan Barichivich,[2] Duncan A. Christie,[2] and Antonio Maldonado[3]

[1] The coastal mountains of semiarid Chile are punctuated by patches of fog-dependent evergreen forests. Fog episodes often occur when the prominent coastal topography intercepts a well developed deck of stratocumulus (Sc) off north central Chile. A 22-year record of ground-based fog observations at Fray Jorge Biosphere Reserve (FJBR, 30°S), atmospheric reanalysis and satellite derived low cloud amount are used to document the annual cycle and interannual variability of fog frequency there. The number of foggy days minimizes during austral winter and then increases rapidly to reach a maximum in spring (the growing season of FJBR trees). The mean annual cycle of the fog-frequency follows closely the annual cycle of the nearby marine Sc amount and lower tropospheric stability (LTS). The springtime fog frequency, nearby marine cloud amount and LTS are also well correlated at interannual timescales. Colder than normal sea surface temperatures and warmer than normal air temperatures aloft near 30°S strengthen the temperature inversion and lead to a more persistent cloud deck and higher than normal fog frequency at FJBR. La Niña years produce temperature anomalies very similar to the pattern described before and consequently they are associated with higher than normal springtime fog frequency at FJBR. Conversely, El Niño years are associated with less foggy conditions at FJBR. Interestingly, El Niño–Southern Oscillation (ENSO) related rainfall anomalies in north central Chile are opposite to ENSO-related anomalies in fog-frequency. We discuss the overall impact of ENSO in FJBR ecosystems as well as the prospects of FJBR in future climate scenarios driven by increased greenhouse gases.

1. Introduction

[2] North central Chile (west coast of South America, Figure 1a) is year-round under the influence of the southeast Pacific (SEP) anticyclone, maintained by large-scale subsidence at subtropical latitudes. This results in very dry and stable conditions, with annual mean rainfall ranging from about 100 mm at 30°S to virtually zero to the north of 25°S along the Atacama desert [e.g., *Houston and Hartley*, 2003]. Despite these dry conditions, patches of diverse plant communities punctuate the coastal mountains of this otherwise arid environment [*Rundel et al.*, 2007; *Armesto et al.*, 2007]. For instance, several spots of *lomas* communities dominated by *Tillandsia* species ("airplants") occur in some coastal hills around 21°S [*Pinto et al.*, 2006]. Farther south there are several isolated forests at the top of the coastal range (400–650 m ASL) dominated by the endemic evergreen tree species *Aextoxicon punctatum* (locally known as *Olivillo* or *Tique*) and other hygrophilous trees, woody wines and ferns. The most prominent of these forests are located around 30°S and are under protection by the Fray Jorge National Park and UNESCO Biosphere Reserve (FJBR, Figures 1b and 1c) given their exceptional biogeographical importance. It is thought that large-scale geological processes during the Pleistocene produced climate changes that gradually segregated these northern relict forests from their continuous range currently located about 1000 km farther south in a region where annual rainfall exceeds 800 mm [*Villagrán and Armesto*, 1980; *Villagrán et al.*, 2004; *Núñez-Avila and Armesto*, 2006]. In situ studies have shown that coastal fog over the mountain tops is the main, if not the only, source of water for the relict forest at FJBR [*Kummerow*, 1966; *del-Val et al.*, 2006] and other plant communities along arid and semiarid Chile [*Larraín et al.*, 2002; *Pinto et al.*, 2006]. Isolated fog-dependent forests (fog-oases) are also found in other arid/semiarid environments around the world, including the relict deciduous forests in the Dhofar mountains in Oman [*Hildebrant and Eltahir*, 2006], laurel forests on Canary island [*Garcia-Santos et al.*, 2004], cloud forests in eastern Mexico [*Vogelmann*, 1973], and relict stands of Bishop and Torrey pine in California [*Fisher and Still*, 2007].

[3] FJBR encompasses a coastal strip between the mouth of the Limari river and the Coquimbo bay. An elongated

[1]Department of Geophysics, Universidad de Chile, Santiago, Chile.
[2]Laboratorio de Dendrocronología, Facultad de Ciencias Forestales, Universidad Austral de Chile, Valdivia, Chile.
[3]Laboratorio de Paleoambientes, Centro de Estudios Avanzados en Zonas Aridas, Universidad de La Serena, La Serena, Chile.

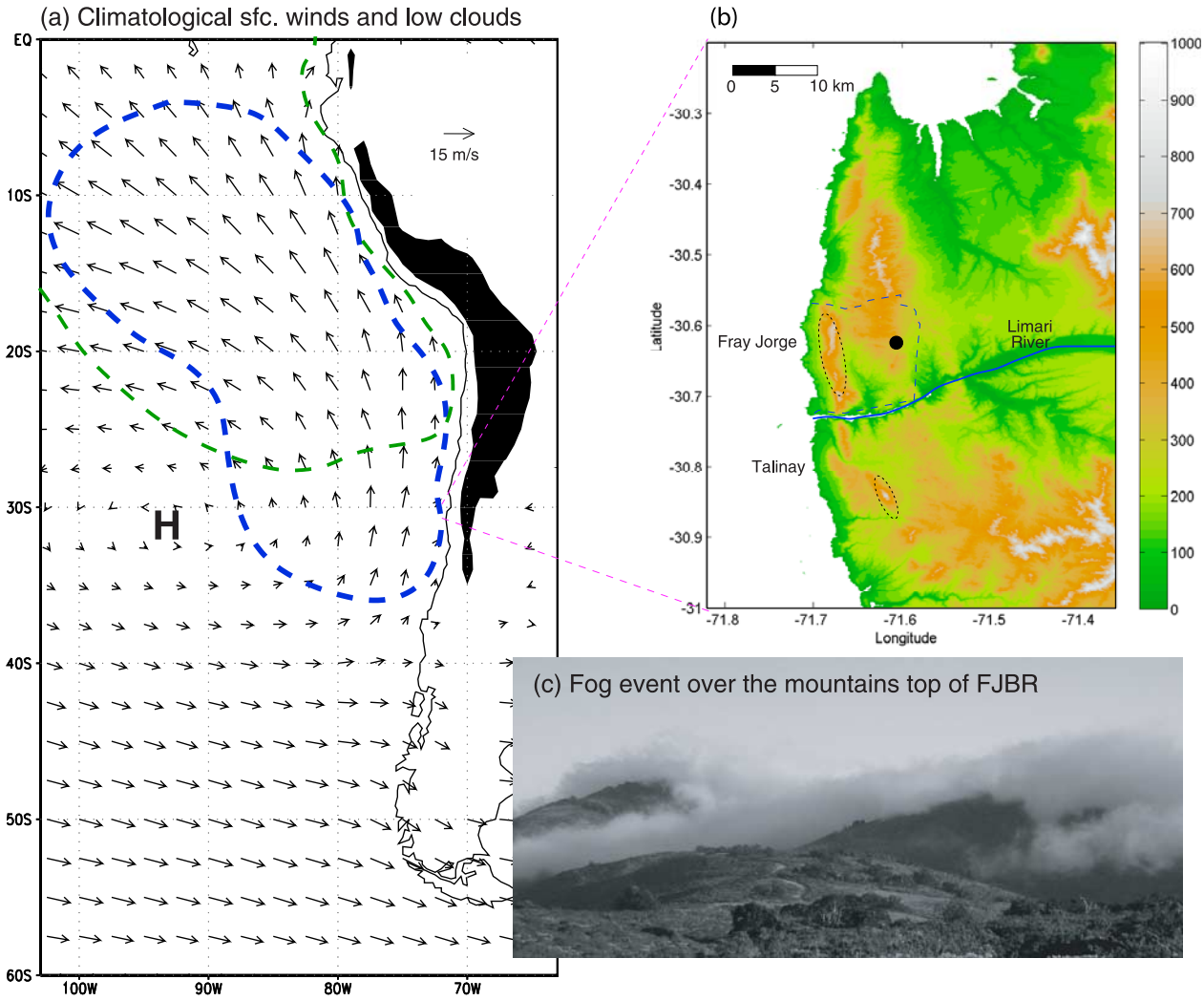

Figure 1. Climatological and geographical setting of Fray Jorge Biosphere Reserve (FJBR). (a) Annual mean surface winds (arrows, scale at top). Letter H indicates the center of the subtropical anticyclone that drives the southerly winds along the Chilean coast. Black area indicates terrain elevation in excess of 3000 m ASL (the central and subtropical Andes). Dashed lines indicate the spatial extent of the stratocumulus cloud deck (cloud fraction larger than 65%) during austral fall/winter (green line) and spring/summer (blue line). (b) Topography of FJBR and adjacent areas (inset in Figure 1a) obtained from the Space Shuttle Topography Mission (90 m horizontal resolution). Color scale in m ASL. The dashed line indicates the Park borders, and the dotted lines outline areas of cloud forest. The solid circle show the location of the FJBR park ranger's station. (c) A fog event at FJBR. The picture was taken from the lowland immediately to the east (inland) of the coastal mountains.

mountain ridge runs parallel to the coastline rising abruptly to its top (between 500 and 700 m ASL) within 10 km of the seashore and decreasing more gently toward an inland plateau (Figure 1b). The cloud forest is located between 500 m ASL and the summit [*del-Val et al.*, 2006] in the seaside of the ridge. FJBR *Olivillo* forest occurs as a mosaic of scattered patches of varying size (0.1–22 ha) with a total area of 86.7 ha [*Squeo et al.*, 2006; *del-Val et al.*, 2006]. Smaller patches tend to be located on the mountain plateau, whereas larger patches are found on steeper slopes facing the ocean, thus having a larger effective area for fog interception. Remarkably, greater water drip inside the forest patches allows for a dense coat of mosses, lichens and liverworts [*Villagrán and Armesto*, 1980; *Squeo et al.*, 2004; *Villagrán et al.*, 2004]. The cloud forest mosaic plays a key role in maintaining the assemblage of animal species of the ecosystem, especially during adverse climatic periods. A high proportion of the species of birds and beetles present in the landscape are restricted exclusively to the forest patches [*Cornelius et al.*, 2000; *Barbosa and Marquet*, 2001]. Patches are used as a refuge by some animal species such as rodents from the semiarid matrix during extremely dry years [*Milstead et al.*, 2007]. *Olivillo* trees act as natural fog collectors but fog-water deposition is highly heterogeneous through the landscape. Typically, fog-water interception is maximum in the windward edges and declines steeply toward the forest interior reaching a minimum in the leeward edge due to a fog-shadow effect [*del-Val et al.*,

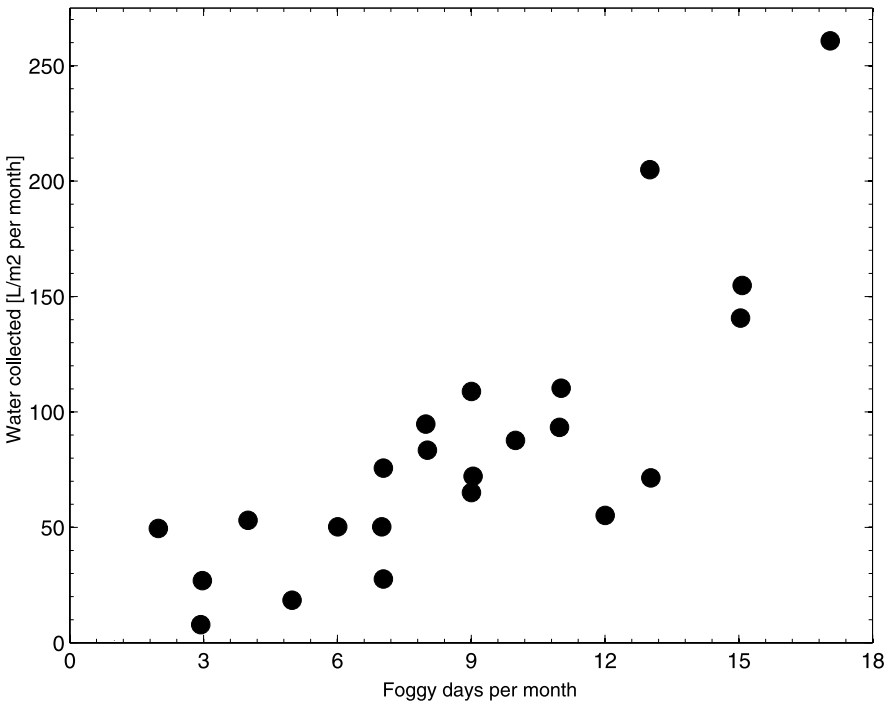

Figure 2. Relationship between the qualitative Fog Index (foggy days per month) at Fray Jorge Biosphere Reserve (FJBR) and cloud-water per month captured by passive fog collectors installed near the top of El Tofo mountains (29.3°S/71.3°W/580 m ASL), about 100 km north of FJBR, from 1989 to 1990.

2006]. Tree regeneration is mainly restricted to the windward edges and it is more abundant in larger than smaller forest patches due to increased fog interception [*del-Val et al.*, 2006]. *Camanchacas*, the Chilean name for fog events in the coastal mountains, also provides potable water to human settlements [*Schemenauer et al.*, 1988].

[4] In general terms, coastal fog along semiarid Chile results from the interception of the nearby marine low clouds by the prominent coastal topography (see section 3). The low-level flow over the ocean is mostly parallel to the coastal topography (i.e., southerly winds) so orographic uplift plays a secondary role in the occurrence of fog over the coastal mountains. The persistent stratocumulus deck off north central Chile is an integral part of a cool, moist marine boundary layer (MBL) over the SEP capped by a strong, subsidence-driven air temperature inversion (e.g., E. Serpetzoglou *et al.*, Boundary layer, cloud, and drizzle variability in the southeast Pacific stratocumulus regime, submitted to *Journal of Climate*, 2008). The spatial distribution of *Camanchacas* is, however, quite complex [*Cereceda and Schemenauer*, 1991; *Cereceda et al.*, 2002] as the synoptic-scale circulation is disturbed by topographically induced mechanical and thermal local-scale effects.

[5] The fog occurrence and cloud water availability along semiarid Chile greatly varies in time scales from diurnal to interannual [*Schemenauer et al.*, 1988; *Larraín et al.*, 2002]. In this work we specifically document the interannual variability of the fog occurrence at FJBR. In contrast with the well documented interannual variability of rainfall in central and northern Chile [*Montecinos and Aceituno*, 2003], this is the first attempt to characterize the interannual variations of fog in this region and to interpret these variations in terms of planetary-scale climate anomalies. Year-to-year changes in water availability are likely to have a profound impact in the fog-dependent ecosystems at FJBR and nearby areas, and they represent the foundation for decadal to centennial variability. As such, results of this study might be useful for biogeoscience studies in semiarid Chile. More detailed analyzes regarding the mesoscale organization of the coastal fog in FJBR, as well as the applicability of our results to other fog oases along semiarid Chile, are beyond the scope of this paper as they require a numerical modeling approach.

[6] The rest of the paper is organized as follows. In section 2 we describe the in situ and global data used in this study. In section 3 we provide an overview of the climatological features along north central Chile that are relevant to the occurrence of fog at FJBR and describe their mean annual cycles. Section 4 documents the year-to-year variability in fog frequency and its dependence on atmospheric conditions at regional (section 4.1) and global (section 4.2) scales. The potential response of FJBR relict forests and ecosystems to changes in fog and rainfall at interannual timescales is discussed in section 5. Section 6 summarizes our main findings.

2. Data

[7] The primary data used in this work are the visual observations taken by park rangers at FJBR headquarters (Figures 1b and 1c) located in the lowlands immediately to the east of the coastal mountains (recall that the forests are in the seaside of the mountains). Three times a day (08:00, 14:00 and 18:00 local time) the rangers look west and determine whether or not a low-level cloud is present over

the mountains. A "foggy-day" is defined as a day in which all three observations indicate presence of fog. A monthly fog index (Φ) is defined as the sum of the foggy days within each calendar month. Φ at FJBR is available for the 22-year period from 1985 to 2006, allowing a reasonable examination of its interannual variability. There are, however, several issues of concern on the Φ definition. First, the basic data are of subjective nature, although the cloud/no-cloud classification is rather unequivocal as the ranger's station has an excellent perspective of the coastal mountain summits. Second, as discussed later in section 3, marine clouds and coastal fog tend to dissipate in the afternoon, especially during summer, and peak at nighttime, when observations are not available. That may introduce a seasonal bias in Φ since foggy days require presence of fog at all three observation times. Unfortunately, we do not have access to all the hourly observations to redefine Φ. Third, given the location of the rangers' station in the lee side of the mountains, our index does not account for those days when the fog is restricted to the forest in the seaside of the mountains. Since Fray Jorge fog-forests exist precisely because the *Camanchacas* tend to last longer there, alternative definitions of foggy days may not result in substantial changes in Φ and we decided to perform our analysis based on this index. To further document the ability of Φ to characterize the fog-occurrence and water availability, Figure 2 shows a scatterplot between monthly values of Φ and cloud-water captured by passive fog-collectors installed at the top of El Tofo mountain (580 m ASL; ~100 km north of FJBR) during the 1989–1990 period [*Cereceda et al.*, 1997], which are strongly positively correlated (r = +0.81).

[8] The large-scale tropospheric circulation is characterized using National Centers for Environmental Prediction–National Center for Atmospheric Research (NCEP-NCAR) reanalysis fields [*Kalnay et al.*, 1996]. Here we used monthly averages of selected fields at the surface and pressure levels on a 2.5° × 2.5° latitude-longitude grid. Monthly mean sea surface temperatures (SST) were obtained from the extended-reconstructed SST data set, also available on a 2.5° × 2.5° latitude-longitude grid, constructed by blending in situ observations and satellite estimates [*Smith and Reynolds*, 2004].

[9] Monthly mean daytime low cloud amount (LCA) was obtained from the International Satellite Cloud Climatology Project (ISCCP) D2 data set [*Rossow and Schiffer*, 1999] for the period 1985–2005. Low-level refers to clouds whose top are at a pressure greater than 680 hPa (below 3000 m ASL) thus capturing the stratocumulus (Sc) coverage (clouds tops around 1000 m ASL). On the other side, the subtropical SE Pacific exhibits a small, if any, frequency of other cloud types [e.g., *Norris*, 1998] so that LCA is an excellent, albeit coarse, proxy of Sc frequency in this area. Cloud amount represents the temporal frequency (% of days within a month) of occurrence of cloudy conditions in individual satellite image pixels. Each pixel covers an area of about 4 to 40 km^2, and was later aggregated to construct LCA on a 2.5° × 2.5° latitude-longitude grid.

3. Climate Background

[10] As noted in the introduction, the climate along the subtropical west coast of South America is largely determined by the presence of the SEP anticyclone and the region's prominent topography (coastal range and the Andes cordillera). The marked subtropical subsidence, the blocking effect of the Andes, and the absence of baroclinic disturbances equatorward of ~30°S are all factors that produce very dry conditions in north central Chile [*Houston and Hartley*, 2003; *Rutllant et al.*, 2003]. The pronounced south-to-north reduction in precipitation is evident in the transect of annual mean rainfall included in the upper panel of Figure 3. At La Serena, a coastal city a few tens of km north of FJBR, the annual rainfall typically (65% of the years) varies between 60 and 100 mm, almost entirely concentrated in wintertime (June–July–August) due to the passage of the subtropical tail of cold fronts. As discussed in more detail in section 4, extremely wet (dry) winters tend to occur during the warm (cold) phase of El Niño–Southern Oscillation (ENSO).

[11] The pressure gradient between the center of the SEP anticyclone (at about 27°S/80°W) and the coast (roughly along 73°W) is in balance with low-level southerly (coastal parallel) winds, which in turn forces upwelling of cold waters due to Ekman transport and pumping [e.g., *Shaffer et al.*, 1999]. The cold SST and the adiabatically warmed air aloft lead to the formation of a very persistent and strong temperature inversion over the SEP [*Garreaud et al.*, 2001; Serpetzoglou et al., submitted manuscript, 2008]. The temperature inversion caps a moist, cool marine boundary layer (MBL) often topped by shallow Sc. Indeed, satellite observations reveal that an extensive deck of Sc blankets most of the SEP [e.g., *Klein and Hartmann*, 1993].

[12] The nearshore structure of the MBL is illustrated in the lower panel of Figure 3 by a transect along the coast of the annual mean cloud base height ($\bar{z}_c$), inversion base height ($\bar{z}_i$) and lifting condensation level (*LCL*), superimposed on a coastal topographic profile (see Appendix A for details on this climatology). The coastal topography is the average of the terrain elevation between the local coastline and a point 15 km eastward (inland). The MBL depth (signaled by $\bar{z}_i$) increases northward, from ~450 m at 33°S to ~1100 m at 22°S, consistent with the sea surface warming along the coast, and so does $\bar{z}_c$ leading to a nearly constant cloud thickness ($\bar{z}_i - \bar{z}_c \sim 200$ m). The mean *LCL* also increases northward but only 250 m in this latitudinal span. Since the difference between $\bar{z}_c$ and *LCL* is indicative of the vertical extent of the mixing within the MBL [e.g., *Albrecht et al.*, 1995] the MBL appears to be fully coupled to the south of about 30°S ($LCL \sim \bar{z}_c$) and becomes increasingly decoupled to the north of this latitude ($LCL \ll \bar{z}_c$). Within the MBL the prevailing winds off north central Chile are parallel to the coast [*Garreaud and Muñoz*, 2005] and there is little (if any) orographic uplift (Figure 1a), emphasizing the role of the Sc deck in the occurrence of coastal fog.

[13] Figure 3 also shows the climatological annual mean, maximum and minimum of low cloud amount off the coast (5° to the west of the coastline). Marine low clouds are quite prevalent off northern Chile, where LCA > 60% year-round. To the south of 30°S the annual mean LCA decreases sharply mostly due to the low frequency of clouds during fall and winter. In that season coastal lows disturb the MBL resulting in Sc clearing with a near weekly periodicity [*Garreaud et al.*, 2002]. Thus, FJBR coastal mountains

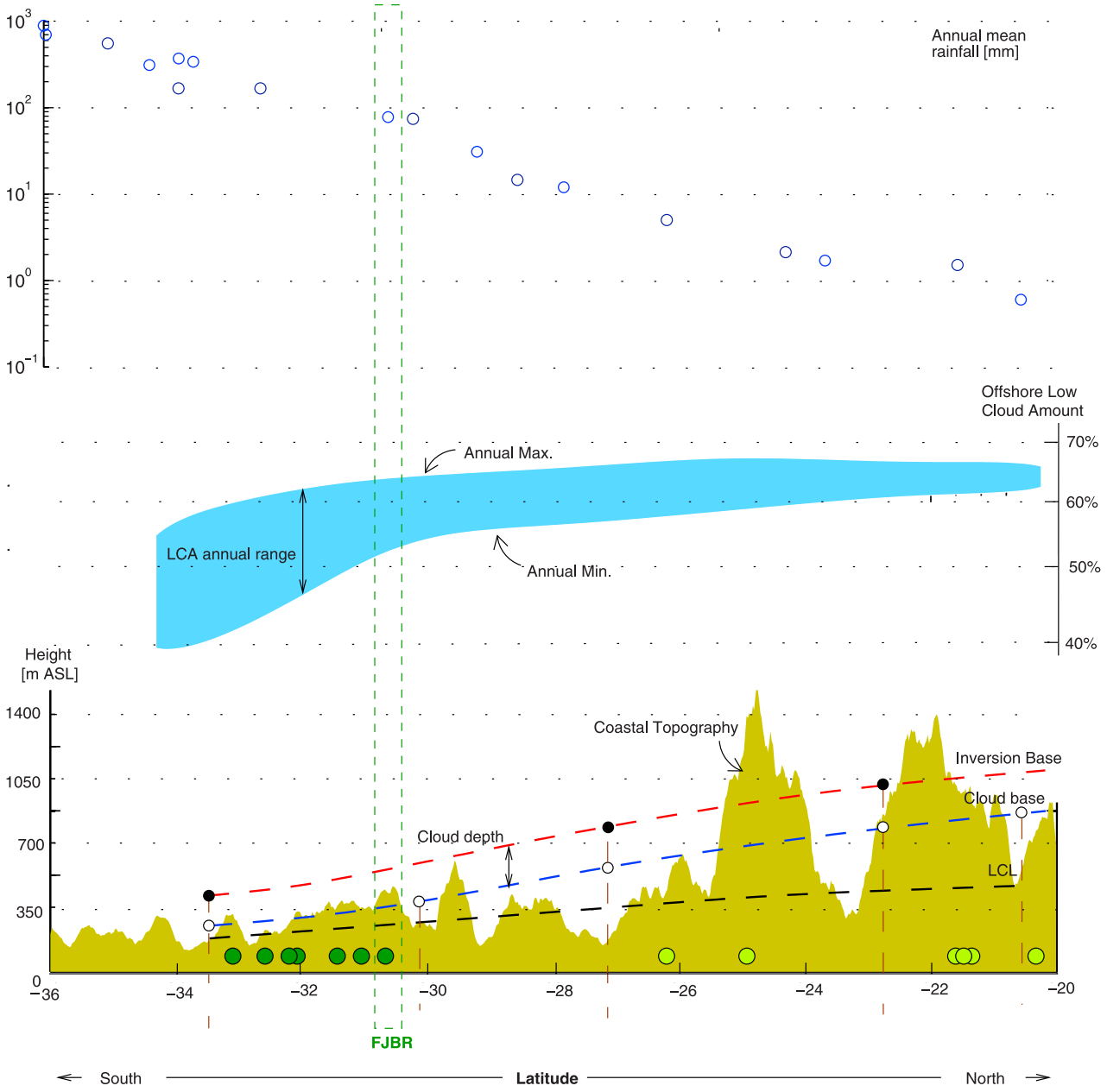

Figure 3. Transect of select meteorological variables along the coast of north central Chile. The green dashed box indicates the latitudinal span of Fray Jorge Biosphere Reserve (FJBR). The upper graph shows the climatological annual mean rainfall at coastal stations. Note that the rainfall scale at left is logarithmic. The light blue area in the middle is bounded by the annual maximum and annual minimum of the ISCCP low cloud amount (LCA in %, scale at right) off the coast. The width of this area indicates the amplitude of the mean annual cycle of the LCA. The yellow area at the bottom is the coastal topographic profile (average height from the coast and a point 15 km inland). Solid circles show the annual mean height of the inversion base at radiosonde stations. The red (black) dashed line is a cubic-spline fit of the inversion base (lifting condensation level, LCL) obtained from radiosonde observation. The blue dashed line is a cubic-spline fit of the cloud base height from ground-based observations (open circles). Dark and light green circles indicate *Aextoxicon punctatum* relict forest and *lomas* communities, respectively. See text for details.

have their top (500–600 m ASL) well into the climatological cloud layer, located in a region of moderate to high prevalence of marine low clouds, and where the MBL tends to be coupled hindering daytime breakup of Sc [*Turton and Nicholls*, 1987]. These regional-scale conditions are clearly favorable for the occurrence of coastal fog in FJBR, although local-scale factors seem to play an important role in the high prevalence of *Camanchacas* there [*Schemenauer et al.*, 1988].

Table 1. Location of Fog-Dependent Coastal Vegetation Communities Along Semiarid Chile[a]

Site Name	Latitude	Reference
Olivillo (Aextoxicon punctatum) Relict Forests		
Cerro Curauma	33.17°S	*Novoa* [2006]
Zapallar	32.55°S	*Villagrán et al.* [2004]
Cerro Iman	32.22°S	*Villagrán et al.* [2004]
Cerro Santa Ines	32.16°S	*Villagrán et al.* [2004]
Huentelauquen	31.50°S	*Villagrán et al.* [2004]
Talinay	30.84°S	*Villagrán et al.* [2004]
Fray Jorge (FJBR)	30.65°S	*Villagrán et al.* [2004]
Airplants (Tillandsia) Lomas Communities		
Site 1	26.10°S	*Thompson et al.* [2003]
Site 2	24.93°S	*Dillon* [1991]
Site 3	21.38°S	*Pinto et al.* [2006]
Chipana	21.20°S	*Pinto et al.* [2006]
Punta Gruesa	20.48°S	*Pinto et al.* [2006]
Alto Patache	20.49°S	*Pinto et al.* [2006]
Site 4	20.20°S	*Pinto et al.* [2006]
Arica sector	18.23°S	*Pinto et al.* [2006]

[a]From south to north.

[14] The coastal transect in Figure 3 also includes the location of *Olivillo* relict forests and *Lomas* communities reported in the literature (see Table 1). Seven *Olivillo* forests are located between 33° and 30°S (being FJBR the northernmost location of them) on the seaside of coastal mountains whose tops reach the climatological cloud base. Between 30°S and 26°S there is a gap in coastal vegetation oases that coincides with a lack of coastal mountains reaching the mean cloud base, with the exception of the El Tofo mountains just north of 30°S. To the north of 26°S several *Lomas* communities, dominated by *Tillandsia* species ("*airplants*"), have been reported on the seaside of coastal hills, whose tops (some in excess of 1000 m ASL) also intercept the climatological cloud base. This figure suggests a strong control of coastal topography and cloud base height upon the location of the vegetation communities in semiarid Chile, although establishing a causal relationship among these variables is beyond the scope of this paper.

[15] The annual cycle of fog occurrence at FJBR is shown in Figure 4 by the long-term mean of Φ. For context, we also included the climatological monthly mean values of LCA and lower tropospheric stability (LTS) just offshore of FJBR (30°S/73°W), as well as rainfall at La Serena. The LTS, defined as the difference in air potential temperature between 700 hPa and the surface (LTS = θ[700 hPa] − θ[surface]), is a rough indicator of the inversion strength

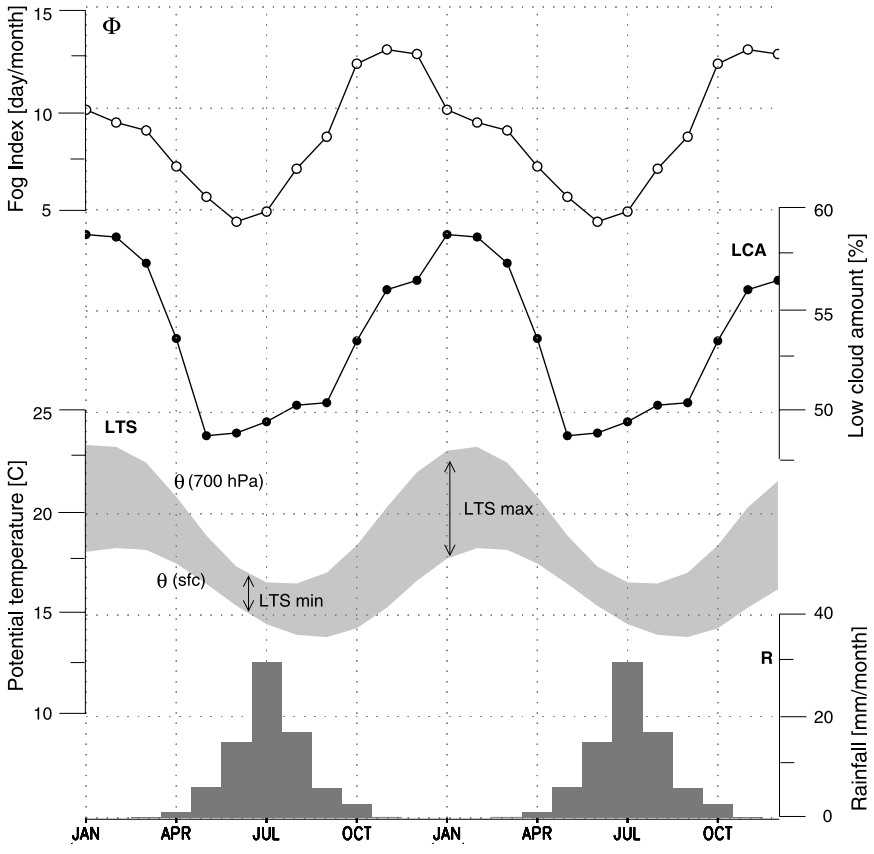

Figure 4. Mean annual cycle of selected variables at or near Fray Jorge Biosphere Reserve (FJBR). For clarity the annual cycle is repeated twice. The variables are the Fog Index at FJBR (upper curve, open circles), ISCCP low cloud amount off FJBR at 30°S/73°W (lower curve, filled circles), 700 hPa potential temperature (upper limit of the shaded area) and surface potential temperature (lower limit of the shaded area) at 30°S/73°W, and rainfall at La Serena (bars). In all cases the mean was calculated using the common period 1985–2006. Note that the width of the shaded area is the lower tropospheric stability LTS = θ[700 hPa] − θ[surface].

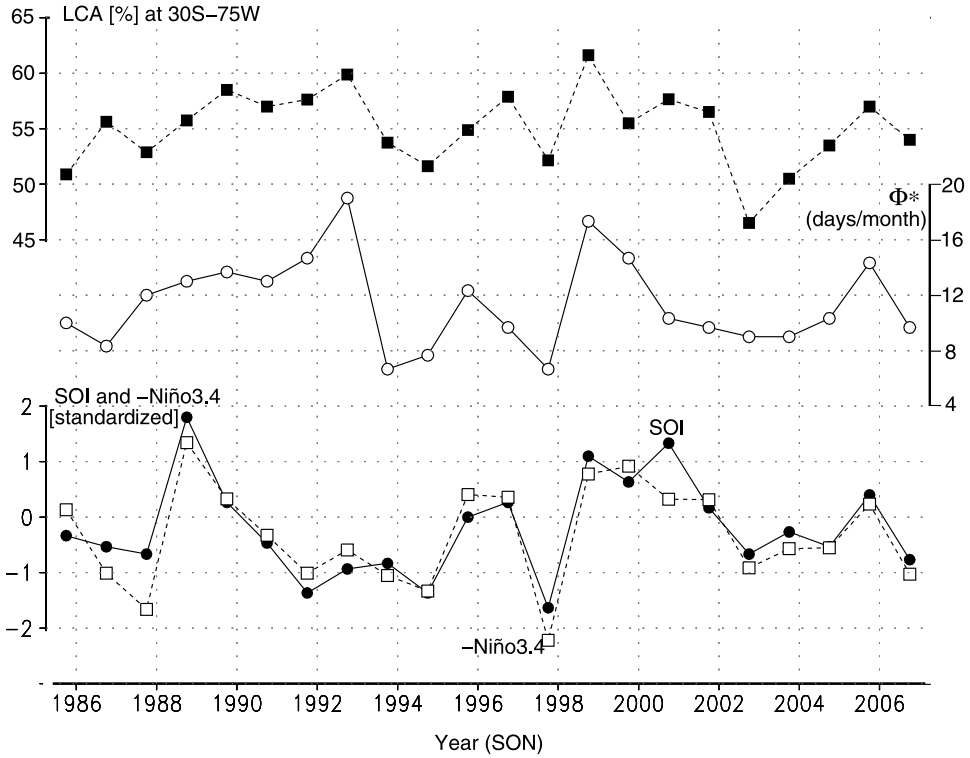

Figure 5. Time series of September–October–November average of the ISCCP low cloud amount at 30°S/75°W (LCA, closed squares, scale at left), Fray Jorge Biosphere Reserve Fog Index (Φ*, open circles, scale at right), the Southern Oscillation Index (SOI, solid circles, scale at left) and the Niño3.4 (open squares, scale at left). Niño3.4 has been inverted.

and correlates positively with Sc cloud amount at sub monthly and seasonal timescales [*Klein and Hartmann*, 1993]. The empirical association between LTS and LCA does not have a robust theoretical foundation [*Wood and Bretherton*, 2004]; nevertheless, it has been proposed that confinement of the moist air at low levels by a "capping" inversion is a prerequisite for the existence of Sc decks. A low LTS value is indicative of a weaker inversion and possibly a deeper, decoupled MBL that make the Sc more susceptible to dissipation [*Klein and Hartmann*, 1993]. Furthermore, simple numerical models of cloud topped, well mixed MBL predict an increase of cloudiness in response to colder SST [e.g., *Schubert et al.*, 1979] and hence higher LTS.

[16] According to the fog index, fog frequency at FJBR is reaching its minimum in winter (4–6 foggy days per month) and increases in early spring to reach a maximum (15 days per month) from October to December. Φ decreases slightly in late summer and further decays during fall. A somewhat similar cycle is observed in offshore cloud amount and LTS, but both variables peak in January. The annual cycle of marine clouds off FJBR is consistent with the seasonal migration of the Sc deck over the SEP, that reaches its southernmost position (off north central Chile) in austral summer and its northernmost position (off Peru) in austral winter [e.g., *Klein and Hartmann*, 1993] (see also Figure 1a). The cloud top and continental daytime heating is more intense in summer, increasing the possibility of cloud dissipation during afternoon [*Rutllant et al.*, 2003; *Muñoz and Garreaud*, 2007]. That may explain why Φ slightly decreases just when the nearby marine Sc reaches a maximum. Also evident in Figure 4 is the wintertime maximum in rainfall, precisely when marine Sc and coastal fog are at a minimum.

4. Interannual Variability

4.1. Regional Scale

[17] We now focus on the interannual variability of Φ*, the fog index averaged from September to November (SON). Spring is not only the season of maximum fog occurrence (Figure 4) but also the growing season of the *Olivillo* trees that populate FJBR [*Gutiérrez et al.*, 2008]. The time series of Φ* is shown in Figure 5; for the 22-year period, $\bar{\Phi}^* = 11.4$ days/month and $\sigma(\Phi^*) = 3.5$ days/month, half the amplitude of the mean annual cycle thus underlying the importance of the year-to-year variations of fog frequency. Figure 5 also shows the time series of SON averaged LCA just offshore (30°S/73°W) which is strongly correlated with Φ* ($r = +0.8$). Although our synoptic experience indicates that *Camanchacas* at FJBR often occur in connection with a well developed Sc deck, the amount of interannual variance of fog frequency explained by marine cloud amount is surprisingly high (65%). The remaining of variance in Φ* could be explained by a variety of other factors, such as changes in the cloud base height. For instance, no *Camanchacas* occur if the cloud base is higher than the mountain tops (about 500 m ASL) regardless of the amount of Sc.

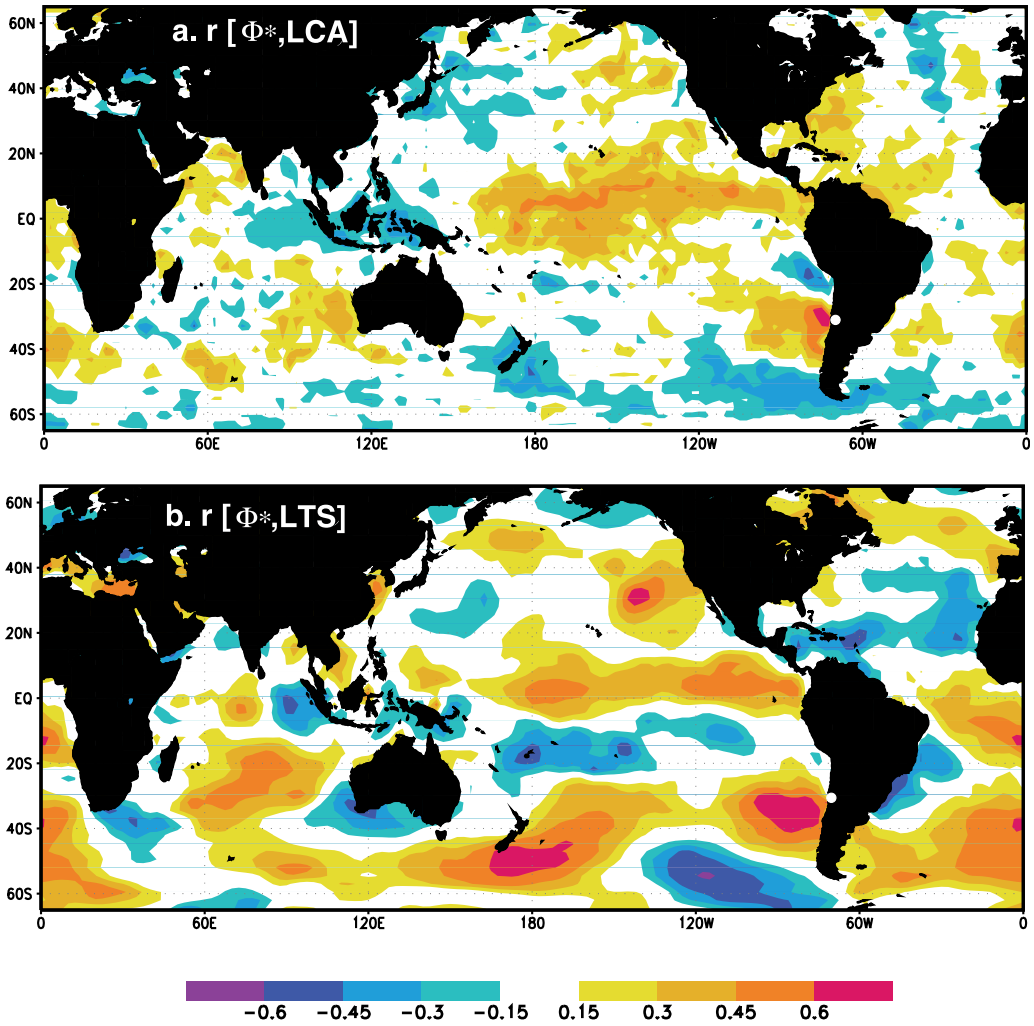

Figure 6. Correlation coefficient between September–October–November (SON) averages of the fog index at FJBR (Φ*) and (a) ISCCP low cloud amount (LCA), and (b) SON average of the lower tropospheric stability (LTS). Only shown are values $|r| \geq 0.15$ which are statistically significant at the 95% confidence level everywhere. The small white circle indicates the position of FJBR at 30°S on the Chilean coast.

[18] To visualize the large-scale patterns of cloudiness and atmospheric circulation simultaneous with fog-frequency anomalies at FJBR, we use 1-point correlation maps. These maps display the correlation coefficient between Φ* and time series of other variables at grid boxes elsewhere over the globe. At each grid box the statistical significance of r(lat,lon) is established using a two-tailed Student's t-test at the 95% confidence level. Figure 6a shows the 1-point correlation map using Φ* and the corresponding SON averaged low cloud amount. As expected from Figure 5, the highest correlations ($r > +0.8$) are found just off FJBR although an area of large correlations extends westward well into open ocean between 25°–40°S. Farther north there is an area of negative correlations. From this we deduce that above (below) normal fog frequencies at FJBR are associated with higher (lower) than normal LCA over the subtropical half of the southeast Pacific Sc deck.

[19] We already showed that the mean annual cycles of coastal fog at FJBR and nearby marine cloudiness follow the mean annual cycle of the lower tropospheric stability (LTS) at a collocated point (Figure 4). The coastal fog/LTS relationship also seems to hold at interannual timescales, as shown by the 1-point correlation between Φ* and the spring average of LTS (Figure 6b). Significant LTS modulation upon Sc amount at monthly and interannual timescales has been previously documented on subtropical oceans [*Klein*, 1997; *Mansbach and Norris*, 2007]. In our case, more than half of the variance of Φ* is explained by year-to-year changes of LTS off central Chile, although the largest correlations are slightly to the south of FJBR. The interannual variability in LTS can in turn be produced by changes in SST or air temperature aloft. Over the SEP, both factors contribute (Figure 7): Φ* is significantly correlated with 700 hPa air temperature (positive values) and SST (negative values).

[20] The correlation pattern in Figure 7a indicates that more (less) foggy conditions at FJBR are associated with colder (warmer) than normal SST all along the west coast of South America, particularly off central Chile. Along this region, SST cooling may result from the strengthening of

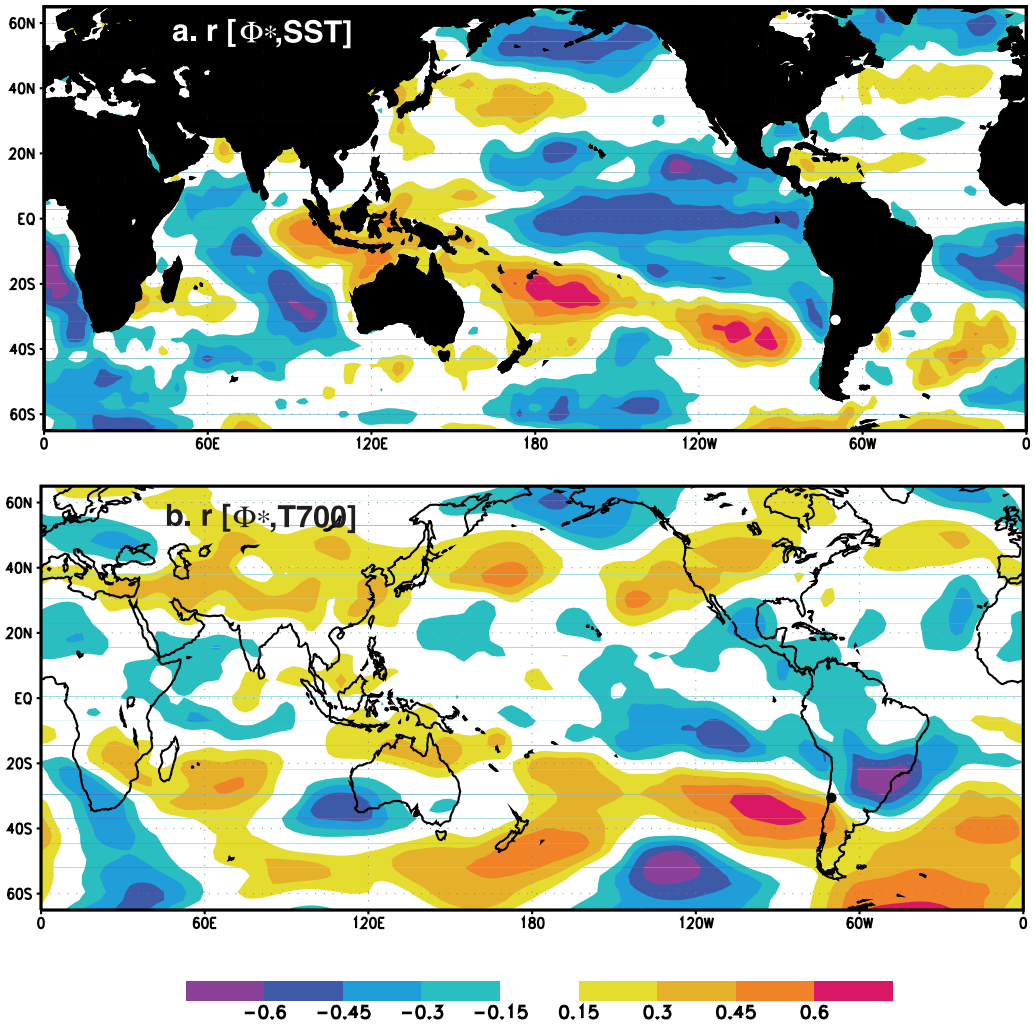

Figure 7. Correlation coefficient between September–October–November (SON) averages of the fog index at FJBR (Φ*) and (a) SON averages of sea surface temperature (SST), and (b) SON average of the 700 hPa air temperature (T700). Only shown are values $|r| \geq 0.15$ which are statistically significant at the 95% confidence level everywhere. The small white circle indicates the position of FJBR at 30°S on the Chilean coast.

the southerly winds that foster more active upwelling [e.g., *Garreaud and Muñoz*, 2005] or the passage of oceanic coastally trapped waves that modulate the position of the thermocline [*Hormazabal et al.*, 2001]. Wind driven cooling seems to be the case here, as inferred from the 1-point correlation between Φ* and the spring average of SLP in Figure 8. The pattern of correlation off the Chilean coast (with a maximum at about 40°S) has strong resemblance with the SLP anomaly pattern that produces strong southerly wind anomalies along the coast at submonthly [*Garreaud and Muñoz*, 2005] and interannual [*Garreaud and Falvey*, 2008] timescales. Under this synoptic setting there is a strong meridional pressure gradient along the Chilean coast. The very steep coastal terrain precludes the development of low-level easterly (cross-shore) flow that would geostrophically balance the meridional pressure gradient; instead, the southerly (along-shore) flow accelerates until turbulent friction in the MBL balance the pressure gradient force. The strengthening of winds within the MBL would also increase the orographic uplift of moist air over the seaside of the FJBR coastal mountains, but as we noted in the climate review, this dynamical effect is likely to be small because the prevailing southerly flow is mostly parallel to the coastal relief.

[21] We are now in position to present a conceptual model of the interannual variability of the fog frequency at FJBR. The driving element is the existence of SLP anomalies off south central Chile and let us assume they are positive. Higher than normal SLP at 30–40°S (i.e., to the south of FJBR) strengthen the southerly wind along the subtropical coast, fostering upwelling of deep waters and hence cooling the MBL. Higher than normal SLP also requires enhanced subsidence at mid levels, warming the free atmosphere. The cooling at low levels and the warming aloft act in concert to increase the inversion strength and its rough indicator (LTS). Therefore, the more effective capping of the moist air within the MBL would lead to higher than normal low level cloudiness over the subtropical SEP and more frequent foggy days at the coastal mountains around 30°S. If we begin the previous conceptual sequence with negative SLP

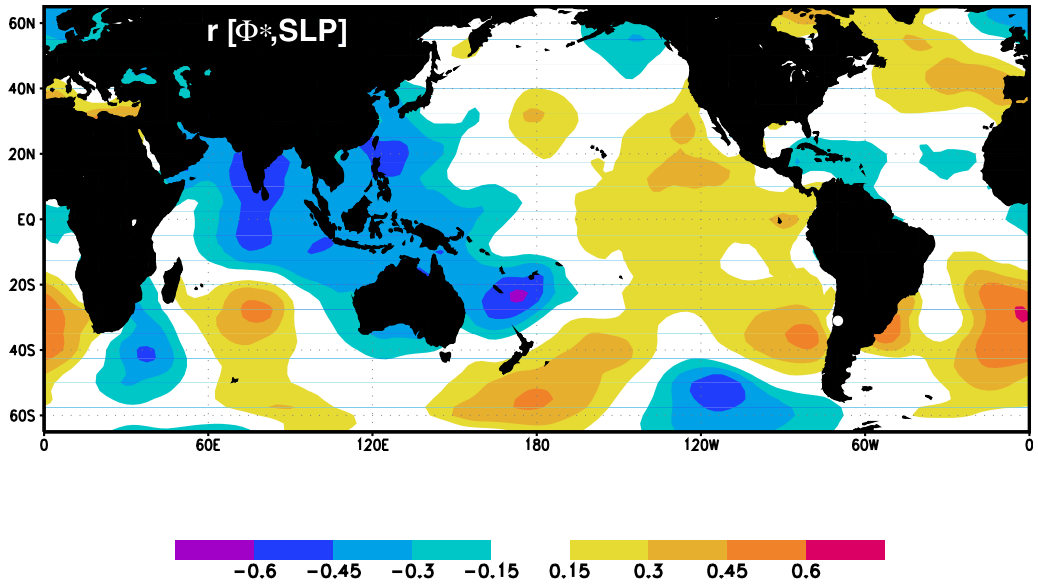

Figure 8. Correlation coefficient between September–October–November (SON) averages of the fog index at FJBR (Φ*) and sea level pressure (SLP). Only shown are values $|r| \geq 0.15$ which are statistically significant at the 95% confidence level everywhere. The small white circle indicates the position of FJBR at 30°S on the Chilean coast.

anomalies we would obtain a decrease in fog occurrence at FJBR.

4.2. Global Scale

[22] Any large-scale circulation mode capable of producing long-lasting (at least seasonal) SLP anomalies off the coast of south central Chile can trigger the conceptual sequence described above and thus modulate the interannual variability of fog frequency at FJBR. There are several of such large-scale modes [e.g., *Kisdon*, 1988, 1991] but the global correlation maps in Figures 6–8 give a clear hint on the most relevant mode in this case. Indeed, the 1-point correlation maps between Φ* and SST/SLP (Figures 7a and 8) are clearly ENSO-like with a polarity such that more (less) foggy conditions at FJBR have a strong resemblance to the canonical La Niña (El Niño) pattern [e.g., *Rasmusson and Carpenter*, 1982; *Yulaeva and Wallace*, 1994]. In addition to the spatial similarities between our 1-point correlation maps and the corresponding ENSO-related SST and SLP anomalies, the time series of fog frequency at FJBR and ENSO index are closely tied. Figure 5 also shows SON averages of Niño3.4 (SST anomalies in the region 5°N–5°S, 120°W–170°W) and

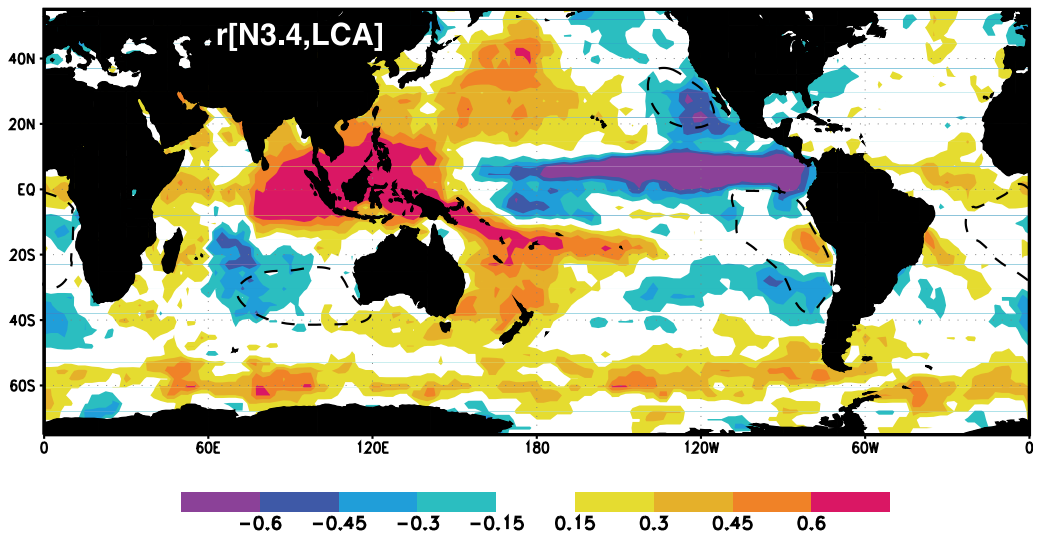

Figure 9. Correlation coefficient between SON averages of the Niño3.4 index and ISCCP low cloud amount (LCA). Only shown are values $|r| \geq 0.15$ which are statistically significant at the 95% confidence level everywhere. The small white circle indicates the position of FJBR at 30°S on the Chilean coast. The dashed lines outline Sc decks over subtropical oceans (LCA > 60%).

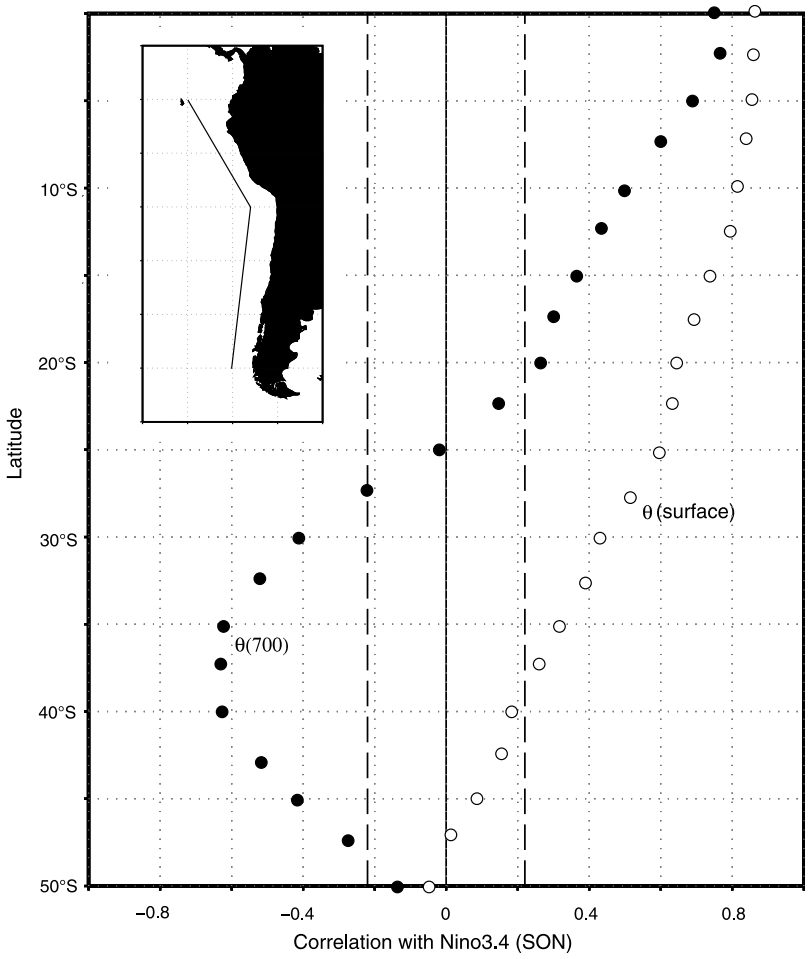

Figure 10. Correlation coefficient between September–October–November (SON) averages of Niño3.4 index and air potential temperature off the coast of South America. The correlations were calculated at the surface (open circles) and the 700 hPa level (solid circles) along the line indicated in the inset. Dashed lines indicate the 99% significance level. The base period is 1970–2005.

the Southern Oscillation Index (SOI) whose correlation with Φ^* are −0.52 and +0.54, respectively.

[23] Using an alternative approach, we regressed the SON seasonal mean of LCA upon Niño3.4 and constructed the corresponding 1-point correlation map shown in Figure 9 (as expected the correlation pattern in Figure 9 is similar to its counterpart in Figure 6a constructed using Φ^*). Over the eastern side of tropical and subtropical oceans, the correlation between Niño3.4 and LCA largely reflects the changes that the Sc deck experiences during the warm and cold phases of ENSO [e.g., *Norris*, 1998; *Deser and Wallace*, 1990; *Park and Leovy*, 2004]. When considering the Sc deck over the SEP (outlined by a dashed line in Figure 9) there is an interesting dipole with the zero line around 20°S such that during El Niño (La Niña) the seasonal Sc coverage increases (decreases) off Peru and northern Chile and decreases (increases) off central Chile. In the southern region, the signal in the marine Sc is passed into the fog frequency at the coast as detected in FJBR.

[24] During austral spring (SON), the control of ENSO on SEP low clouds occurs, at least partially, through local changes in LTS. Figure 10 shows the correlation between SON average of Niño3.4 and air potential temperature along the west coast of South America. At the surface, the correlations are positive and significant from the equator down to 40°S. At 700 hPa the sign of the correlation changes at about 25°S from positive to negative. Let us consider an El Niño; to the south of ∼30°S the combination of warmer than normal SST and colder than normal air at 700 hPa weakens the temperature inversion and, accordingly, reduce the amount of Sc. To the north of ∼25°S, both SST and 700 hPa air temperature increase, but as the signal in air potential temperature amplifies upward, the net result is an increase in LTS and consequently an increase in Sc coverage. The opposite condition occurs during La Niña, featuring a increase (decrease) of Sc to the south (north) of 25°S.

5. Implications for the FJBR Ecosystem

[25] The influence of ENSO on the rainfall regime in central Chile has been known for a long time [e.g., *Aceituno*, 1988]. During El Niño years, the weakening of the SEP subtropical high, the establishment of a blocking anticyclone to the west of the Antarctic peninsula and the stronger than normal subtropical jet aloft produce an equatorward shift of

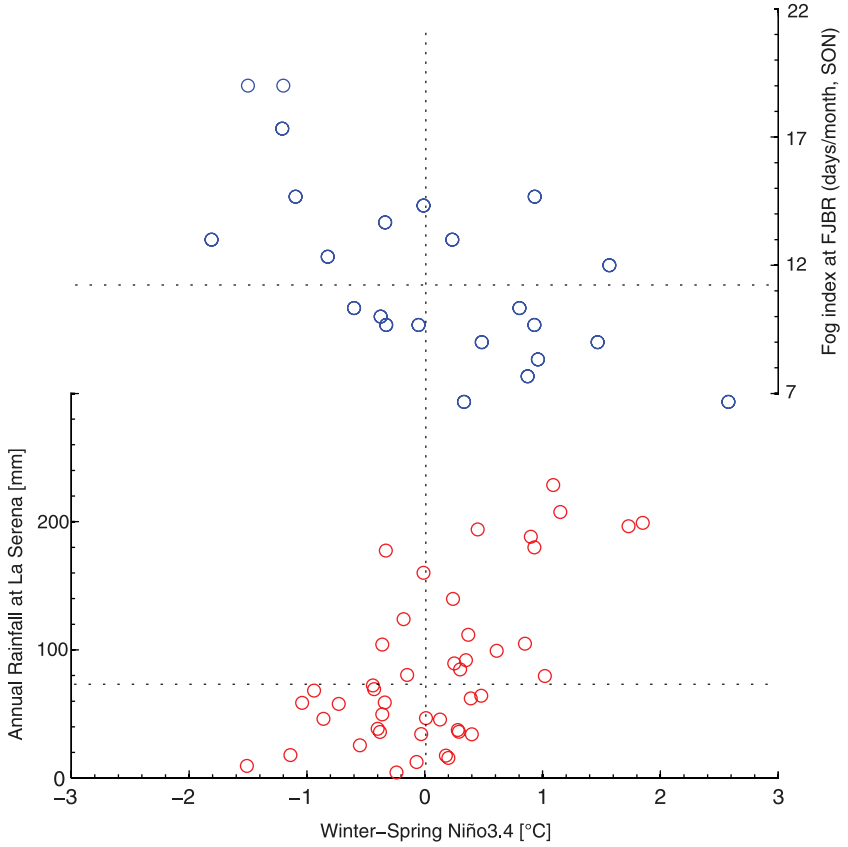

Figure 11. Scatterplot of annual rainfall at La Serena (red circles, 45 years) and springtime fog index at FJBR (blue circles, 22 years) against Niño3.4 values. The fog index is the average number of foggy days during spring (expressed in number of days per month). The Niño3.4 values are the average of monthly values between June and November. Horizontal dotted lines indicate the long-term average of rainfall and fog-index.

the storm track over the south Pacific leading to a more frequent passage of cold fronts over central Chile during wintertime. Consistently, El Niño years are well associated with above normal precipitation in the region 30°–35°S as measured by rain gauge stations along the coast and the central valley [*Montecinos and Aceituno*, 2003] and snow depth records in the Andes [*Masiokas et al.*, 2006]. Conversely, rainfall and snow accumulation tend to be below normal during La Niña years. During neutral years (−0.5°C ≤ Niño3.4 ≤ +0.5°C) precipitation in central Chile is rather randomly distributed between very dry and moderately wet conditions [*Montecinos and Aceituno*, 2003].

[26] The El Niño-wet/La Niña-dry relationship accounts for most of the interannual rainfall variability in the semiarid region around 30°S, including FJBR, and even into the southern edge of the Atacama desert [*Lima et al.*, 1999]. Figure 11 shows the scatterplot of annual rainfall at La Serena and Niño3.4. The correlation coefficient between the two series is 0.76 (significant at the 99% confidence level) and all years within the upper 10% of the rainfall distribution (>180 mm/a) occurred when Niño3.4 > +0.5°C. In this region nearly all precipitation is concentrated in winter (JJA) except for a few episodes in late fall or early spring.

[27] As reviewed by *Holmgren et al.* [2001], high rainfall during El Niño years has a significant and complex, impact upon ecosystem dynamics in semiarid Chile. For instance, in the arid fog-free lowlands shrub community of FJBR (below the forest patches) the seed bank density increased 5- to 10-fold during the 1991–92 El Niño event relative to the dry previous years leading to a "blooming desert" [*Gutiérrez and Meserve*, 2003; *Squeo et al.*, 2006]. The increase in primary productivity of the shrub community resulted in large bottom-up increases of seeds and herb consumers and, later on, top predators [*Meserve et al.*, 2003; *Milstead et al.*, 2007]. In contrast, preliminary tree ring studies in the fog-forests of FJBR demonstrated that tree growth is not correlated with local precipitation occurring during the growing year, and has only marginal positive correlation with rainfall of the previous growing year [*Gutiérrez et al.*, 2008]. This lack of correlation between rainfall and tree growth might be explained as follows. Even during strong El Niño years rainfall does not exceed 250 mm in the FJBR region, well below the annual average that characterize the main range of *Aextoxicon punctatum* forests (>700 mm/a). Further, only a small fraction (less than 20%) of this extra precipitation occurs during the growing season (spring and early summer) of the forest and hardly could compensate the deficit of fog-water interception that occurs during the spring season of an El Niño year, thus leading to below normal water input for the *Olivillo* forests at FJBR. In contrast, during La Niña, there are generally drier conditions during winter but the higher frequency of coastal fog during

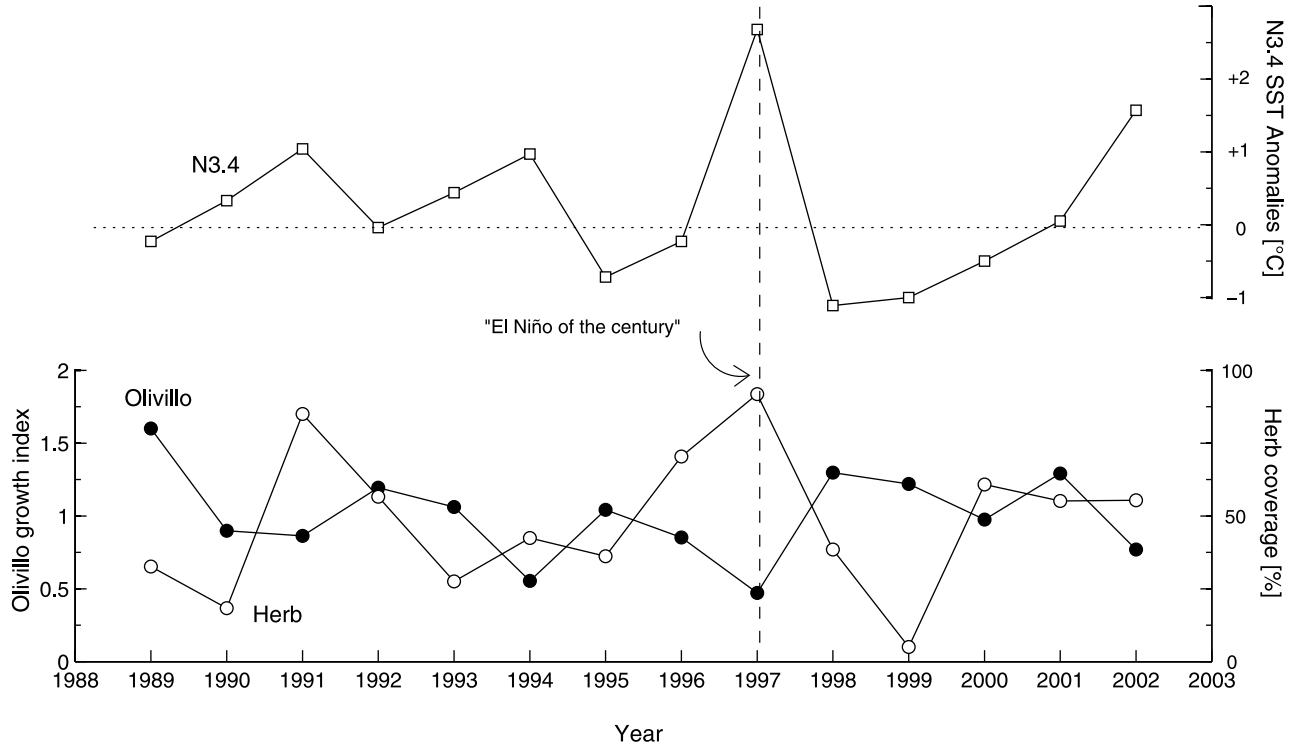

Figure 12. Time series of September–October–November (SON) averages of Niño3.4 index, geophytic plant species coverage at FJBR lowland drylands [from *Gutiérrez et al.*, 2005], and *Olivillo* tree growth index at Santa Ines relict forest, a coastal site at 32.1°S, 150 km south of FJBR [from *Barichivich and Maldonado*, 2007].

spring would produce favorable conditions for forest growth at FJBR.

[28] Therefore, we hypothesize that year-to-year variations in tree growth would be largely determined by interannual variations in fog frequency, which in turn are related with ENSO in a El Niño-less fog/La Niña-more fog pattern (Figure 11). This ENSO-related effect on fog-dependent forests is the inverse of its counterpart on rain-dependent shrubland ecosystem. Ecological evidence gives support to this hypothesis, as shown in Figure 12 by the time series of SON averaged Niño3.4 SST anomalies, *Olivillo* tree growth index at Santa Ines relict forest and annual geophytic plant species cover at FJBR lowland drylands [*Gutiérrez et al.*, 2005]. Santa Ines (32°S) is another coastal forest about 150 km to the south of FJBR, but still within semiarid Chile, from where a robust *Olivillo* chronology has been recently developed [*Barichivich and Maldonado*, 2007]. They obtained two increment cores from 25 trees and used standard dendrochronological procedures for processing all the samples and to develop a tree ring width index. Their *Olivillo* tree growth index has a significant correlation with our FJBR SON fog index (r = +0.61). Over the 1989–2002 common period, Niño3.4 appears negatively correlated with *Olivillo* (r = −0.73) and positively correlated with herb coverage (r = +0.58), both statistically significant at the 99% confidence level. As expected, *Olivillo* growth and geophytic plant species cover are inversely correlated (r = −0.49). Particular relevance has the large swings of these two vegetation index around the big El Niño event of 1997 and the subsequent intense La Niña event of 1998. *Barichivich and Maldonado* [2007] also found a persistent antiphase since 1880 between highly correlated oscillatory modes of the Niño3.4 SST anomalies and *Olivillo* growth at ∼5.5 years.

[29] To close this section, let us consider the prospects of FJBR ecosystem persistence in a future climate scenario driven by an increase of anthropogenic greenhouse gases. *Fuenzalida et al.* [2007] analyzed outputs from selected coarse global circulation models (GCMs) and a high-resolution regional climate model under present-day conditions (1970–2000) and the 2070–2100 time period under the IPCC A2 scenario [*Nakicenovic and Swart*, 2000]. It is worth noting that A2 is the IPCC scenario with the second largest atmospheric CO_2 concentration by the end of the century (about 820 ppb) and hence a condition in which regional climate changes (if any) appears clearly. These model-based projections for the end of the 21st century show a slight decrease in precipitation along the coast of north central Chile. There is also a significant increase in the southerly flow along the Chilean coast instigated by a strengthening of the subtropical anticyclone over the SEP [*Garreaud and Falvey*, 2008]. A likely outcome of the stronger winds is a sea surface cooling; in fact, the geographic pattern of surface air temperature change predicted by GCMs show an area of minimum warming over the SEP [*Garreaud and Falvey*, 2008]. The "relative" near-surface cooling and the more rapid warming of the free troposphere lead to an increase of the LTS around 30°S, and eventually to an increase of the coastal fog frequency. In essence, the projected regional climate of the end of the 21st century

looks very much similar to La Niña conditions, with opposite impacts for fog-dependent forests and rainfall-dependent herbs and other plant communities. There are, however, complex biological interactions among both habitats [*del-Val et al.*, 2007; *Milstead et al.*, 2007], so that a more conclusive picture of the potential changes in the ecosystems of FJBR (and the semiarid coast of Chile in general) require further research based on comprehensive meteorological and environmental in situ data as well as coupled atmosphere-biosphere models.

6. Concluding Remarks

[30] A 22-year long record of human, ground-based fog observations at FJBR has allowed us to document the annual cycle and interannual variability of fog frequency in these coastal mountains of semiarid Chile. Atmospheric reanalysis, gridded SST and satellite-derived low cloud amount were used to provide a large-scale context to the local observations at FJBR. The number of foggy days is minimum ($\sim$5 days/month) during austral winter (JJA) and then increases rapidly to reach a maximum (up to 10 days/month) in spring (SON) followed by a gentle decrease during summer and fall. The mean annual cycle of the fog-frequency follows closely the annual cycle of the nearby marine stratocumulus cloud amount, and our synoptic experience indicate that *Camanchacas* at FJBR are often associated with well defined Sc deck off north central Chile. The shallow, low-lying Sc over the southeast Pacific is an integral part of the marine boundary layer, capped by a strong temperature inversion and maintained by large-scale tropospheric subsidence. Indeed, the annual cycle of the cloud amount is largely explained by the annual cycle of lower tropospheric stability, a rough indicator of the inversion strength and its ability to confine the moist, cool air within the MBL.

[31] Fog occurrence at the coastal mountains also depends on local factors and the vertical position of the marine clouds. Yet, 65% of its interannual variance is explained by simultaneous changes in nearby low cloud amount (LCA). The year-to-year coastal cloud/fog variations are in turn well related to changes in lower tropospheric stability. Spring seasons with higher than normal fog frequencies at FJBR are thus associated with colder than normal SST and warmer than normal air temperatures in the middle troposphere (around 700 hPa) around 30°S. Conversely, seasons with lower than normal frequencies are associated with warmer SST and colder air aloft.

[32] At interannual timescales, this temperature dipole in the lower-troposphere off central Chile manifests very clearly during the extreme phases of the ENSO cycle coupled with the sea level pressure (SLP) pattern. During La Niña conditions positive SLP anomalies prevail over the southeast Pacific. The later drives stronger than normal southerly winds along the Chilean coast fostering active upwelling of cold waters and hence cooling the surface air. Higher than normal SLP also requires enhanced subsidence at mid levels, warming the free atmosphere. The cooling at low levels and the warming aloft act in concert as to increase the inversion strength (LTS) leading to more frequent foggy conditions at FJBR. Exactly the opposite signs apply during El Niño, leading to less foggy conditions at FJBR. This relationship between ENSO and fog frequency at FJBR not only emerge in our spatial analysis, but also appears in the linear correlations between the SON averages of the fog index with SOI ($r = +0.54$) and Niño3.4 ($r = -0.52$). More generally, during austral spring (SON), La Niña (El Niño) conditions are associated with more (less) low cloud amount over the subtropical portion of the SEP deck of Sc. To the north of $\sim$25°S the pattern reverses: higher (lower) than normal cloud amount occurs during El Niño (La Niña).

[33] Since coastal fog over the mountain tops is the main, if not the only, source of water for the relict forest at FJBR, year-to-year variations in tree growth should be largely determined by interannual variations in fog frequency, which in turn are related with ENSO in a El Niño-less fog/La Niña-more fog pattern. This ENSO-related effect on fog-dependent forests is the inverse of its counterpart on rain-dependent shrubland ecosystem. Indeed, time series of *Olivillo* radial-growth at Santa Ines forest (another relict forest about 150 south of FJBR) exhibit a negative correlation with Niño3.4 ($r = -0.73$) and annual geophytic plant species coverage ($r = -0.49$) at FJBR.

Appendix A

[34] The climatological values of the cloud base ($\bar{z}_c$) are reported by *Quintana and Berrios* [2007] on the basis of human, ground-based observations at 12 UTC (08:00 local time). The climatological values of the inversion base ($\bar{z}_i$) and the lifting condensation level (*LCL*) were obtained from daily radiosonde data at 12 UTC at Antofagasta (23°S, 1979–2005) and Quintero (33°S, 1979–1998). Daily values of $\bar{z}_i$ were derived from the temperature profile using an objective procedure described by *Morgan and Bornstein* [1977] and LCL = $(T^1 - T_d^1)/8$ where T^1 and T_d^1 are the air temperature and dew point at the first sounding level. Recall that LCL is the level at which a cloud should form provided that the mechanical forcing is enough to lift the near-surface air up to that level and that condensation nuclei are abundant enough for the initialization of condensation. The averaging was restricted to days with 100 m $\leq \bar{z}_i \leq$ 2000 m, a condition that is satisfied around 55% of the time in Quintero and 90% of the time in Antofagasta. We complemented these climatological values with a few observations at 30°S [*Khodayar et al.*, 2007] and 27°S [*Garreaud et al.*, 2001; Serpetzoglou et al., submitted manuscript, 2008], and for visualization purposes were interpolated using cubic splines.

[35] **Acknowledgments.** We are grateful to Pilar Cereceda for providing the El Tofo fog-water record and CONAF IV Región-Chile (Chilean Forest Service) for the Fray Jorge fog record. R.G. is supported by CONICYT (Chile) grant ACT-19. A.M. is supported by FONDECYT (Chile) grant 11070016.

References

Aceituno, P. (1988), On the functioning of the Southern Oscillation in the South American sector. Part I: Surface climate, *Mon. Weather Rev.*, *116*, 505–524.

Albrecht, B. A., C. S. Bretherton, D. Johnson, W. H. Schubert, and A. S. Frisch (1995), The Atlantic Stratocumulus Transition Experiment ASTEX, *Bull. Am. Meteorol. Soc.*, *76*, 889–904.

Armesto, J. J., M. K. Arroyo, and L. Hinojosa (2007), The Mediterranean environment of central Chile, in *The Physical Geography of South America*, edited by T. T. Veblen et al., pp. 184–199, Oxford Univ. Press, New York.

Barbosa, O., and P. A. Marquet (2001), Effects of forest fragmentation on the beetle assemblage at the relic forest of Fray Jorge, Chile, *Oecologia*, *132*, 296–306.

Barichivich, J., and A. Maldonado (2007), Tree growth variability and influences of coastal fog and rainfall in a relict fog-dependent forest in semiarid Chile, paper presented at 4th International Conference on Fog, Fog Collection and Dew, La Serena, Chile, 22–27 July.

Cereceda, P., and R. S. Schemenauer (1991), The occurrence of fog in Chile, *J. Appl. Meteorol.*, *30*, 1097–1155.

Cereceda, P., R. S. Schemenauer, and F. Velásquez (1997), Variación temporal de la niebla en El Tofo, Chungungo, Región de Coquimbo, Chile, *Rev. Geogr. Norte Grande*, *24*, 191–193.

Cereceda, P., P. Osses, H. Larrain, M. Farias, M. Lagos, R. Pinto, and R. S. Schemenauer (2002), Advective, orographic and radiation fog in the Tarapacá region, Chile, *Atmos. Res.*, *64*, 261–271.

Cornelius, C., H. Cofré, and P. A. Marquet (2000), Effects of habitat fragmentation on bird species in a relict temperate forest in semiarid Chile, *Conserv. Biol.*, *1*, 534–543.

del-Val, E., J. J. Armesto, O. Barbosa, D. A. Christie, A. Gutiérrez, C. Jones, P. Marquet, and K. Weathers (2006), Rain forest islands in the Chilean semiarid region: Fog-dependency, ecosystem persistence and tree regeneration, *Ecosystems*, *9*, 1–13.

del-Val, E., J. J. Armesto, O. Barbosa, and P. A. Marquet (2007), Effects of herbivory and patch size on tree seedling survivorship in a fog-dependent coastal rainforest in semiarid Chile, *Oecologia*, *153*, 625–632.

Deser, C., and J. M. Wallace (1990), Large-scale atmospheric circulation features of warm and cold episodes in the tropical Pacific, *J. Clim.*, *3*, 1254–1281.

Dillon, M. O. (1991), A new species of Tillandsia (Bromeliaceae) from the Atacama Desert of northern Chile, *Brittonia*, *43*, 11–16.

Fisher, D., and C. Still (2007), Evaluating patterns of fog water deposition and isotopic composition on the California Channel Islands, *Water Resour. Res.*, *43*, W04420, doi:10.1029/2006WR005124.

Fuenzalida, H., M. Falvey, M. Rojas, and R. Garreaud (2007), Regional climate scenarios for continental Chile, final report, Dep. of Geophys., Univ. de Chile, Santiago. (Available at http://www.dgf.uchile.cl/PRECIS)

Garcia-Santos, G., M. Marzol, and G. Aschan (2004), Water dynamics in a laurel montane cloud forest in Garajonay National Park (Canary Islands, Spain), *Hydrol. Earth Syst. Sci.*, *8*, 1065–1157.

Garreaud, R., and M. Falvey (2008), The coastal winds off western subtropical South America in future climate scenarios, *Int. J. Climatol.*,in press.

Garreaud, R., and R. Muñoz (2005), The low-level jet off the subtropical west coast of South America: Structure and variability, *Mon. Weather Rev.*, *133*, 2246–2261.

Garreaud, R., J. Rutllant, J. Quintana, J. Carrasco, and P. Minnis (2001), CIMAR-5: A snapshot of the lower troposphere over the Southeast subtropical Pacific, *Bull. Am. Meteorol. Soc.*, *82*, 2193–2207.

Garreaud, R., J. Rutllant, and H. Fuenzalida (2002), Coastal lows in north central Chile: Mean structure and evolution, *Mon. Weather Rev.*, *130*, 75–88.

Gutiérrez, A. G., O. Barbosa, D. A. Christie, E. del-Val, H. Ewing, C. Jones, P. Marquet, K. Weathers, and J. J. Armesto (2008), Regeneration patterns and persistence of the fog-dependent Fray Jorge forest in semiarid Chile during the past two centuries, *Global Change Biol.*, *14*, 161–176.

Gutiérrez, J. R., and P. L. Meserve (2003), El Niño effects on soil seed bank dynamics in north central Chile, *Oecologia*, *134*, 511–517.

Gutiérrez, J., P. Meserve, and D. Kelt (2005), Estrcutura y dinamica de la vegetacion del ecosistema semiarido del Parque Nacional Fray Jorge entre 1989 y 2002, in *Historia Natural del Parque Nacional Bosque Fray Jorge*, edited by F. Squeo, J. Gutiérrez, and I. Hernandez, pp. 115–134, Ediciones de la Univ. de La Serena, La Serena, Chile.

Hildebrant, A., and A. B. Eltahir (2006), Forest on the edge: Seasonal cloud forest in Oman creates its own ecological niche, *Geophys. Res. Lett.*, *33*, L11401, doi:10.1029/2006GL026022.

Holmgren, M., M. Scheffer, E. Ezcurra, J. R. Gutiérrez, and G. M. J. Mohren (2001), El Niño effects on the dynamics of terrestrial ecosystems, *Trends Ecol. Evol.*, *16*, 89–94.

Hormazabal, S., G. Shaffer, J. Letelier, and O. Ulloa (2001), Local and remote forcing of sea surface temperature in the coastal upwelling system off Chile, *J. Geophys. Res.*, *106*(C8), 16,657–16,672.

Houston, J., and A. Hartley (2003), The central Andean west-slope rainshadow and its potential contribution to the origin of hyper-aridity in the Atacama Desert, *Int. J. Climatol.*, *23*, 1453–1464.

Kalnay, E., et al. (1996), The NCEP/NCAR 40-years reanalysis project, *Bull. Am. Meteorol. Soc.*, *77*, 437–472.

Khodayar, S., N. Kalthoff, M. Fiebig-Wittmaack, and M. Kohler (2007), Evolution of the atmospheric boundary-layer structure of an arid Andes Valley, *Meteorol. Atmos. Phys.*, *7*, 41–60.

Kisdon, J. (1988), Interannual variations in the Southern Hemisphere circulation, *J. Clim.*, *1*, 1177–1198.

Kisdon, J. (1991), Intraseasonal variations in the Southern Hemisphere circulation, *J. Clim.*, *4*, 939–953.

Klein, S. (1997), Synoptic variability of low-cloud properties and meteorological parameters in the subtropical trade wind boundary layer, *J. Clim.*, *10*, 2018–2039.

Klein, S. A., and D. L. Hartmann (1993), The seasonal cycle of low stratiform clouds, *J. Clim.*, *6*, 1587–1606.

Kummerow, J. (1966), Aporte al conocimiento de las condiciones climáticas del bosque de Fray Jorge, *Bol. Tëc, Fac. Agron. Univ. Chile*, *24*, 21–24.

Larraín, H., F. Velásquez, P. Cereceda, R. Espejo, R. Pinto, P. Osses, and R. S. Schemenauer (2002), Fog measurements at the site Falda Verde north of Chañaral compared with other fog stations of Chile, *Atmos. Res.*, *64*, 273–284.

Lima, M., P. A. Marquet, and F. M. Jaksic (1999), El Niño events, precipitation patterns and rodent outbreaks are statistically associated in semiarid Chile, *Ecography*, *22*, 213–218.

Mansbach, D., and J. R. Norris (2007), Low-level cloud variability over the equatorial cold tongue in observations and models, *J. Clim.*, *20*, 1555–1570.

Masiokas, M., R. Villalba, B. Luckman, C. Le Quesne, and J. C. Aravena (2006), Snowpack variations in the central Andes of Argentina and Chile, 1951–2005: Large-scale atmospheric influences and implications for water resources in the region, *J. Clim.*, *19*, 6334–6352.

Meserve, P. L., D. A. Kelt, B. Milstead, and J. R. Gutiérrez (2003), Thirteen years of shifting top-down and bottom-up control, *BioScience*, *53*, 633–646.

Milstead, W. B., P. L. Meserve, A. Campanella, M. A. Previtali, D. A. Kelt, and J. R. Gutiérrez (2007), Spatial ecology of small mammals in north central Chile: Role of precipitation and refuges, *J. Mammal.*, *88*, 1532–1538.

Montecinos, A., and P. Aceituno (2003), Seasonality of the ENSO-related rainfall variability in central Chile and associated circulation anomalies, *J. Clim.*, *16*, 281–296.

Morgan, T., and R. D. Bornstein (1977), Inversion climatology at San Jose, California, *Mon. Weather Rev.*, *105*, 653–656.

Muñoz, R., and R. Garreaud (2007), The coastal boundary layer diurnal cycle along north central Chile, paper presented at 7th Conference on Coastal Atmospheric and Ocean and Prediction and Processes, Am. Meteorol. Soc., San Diego, Calif., 10–13 Sept.

Nakicenovic, N., and R. Swart (Eds.) (2000), *Special Report on Emissions Scenarios*, Cambridge Univ. Press, New York.

Norris, J. (1998), Low cloud type over the ocean from surface observations. Part II: Geographical and seasonal variations, *J. Clim.*, *11*, 383–403.

Novoa, P. (2006), Hallazgo de bosque *Aextoxicon punctatum*, Aextoxicaceae, familia endémica monoespecífica de Chile, en el Cerro Curauma, Valparaíso, Libreta Botánica. (Available at http://botanicaler.blogspot.com)

Núñez-Avila, M. C., and J. J. Armesto (2006), Relict islands of the temperate rainforest tree *Aextoxicon punctatum* (*Aextoxicaceae*) in semi-arid Chile: Genetic diversity and biogeographic history, *Aust. J. Bot.*, *54*, 733–743.

Park, S., and C. Leovy (2004), Marine low-cloud anomalies associated with ENSO, *J. Clim.*, *17*, 3448–3469.

Pinto, R., I. Barria, and P. A. Marquet (2006), Geographical distribution of Tillandsia lomas in the Atacama Desert, northern Chile, *J. Arid Environ.*, *65*, 543–552.

Quintana, J., and P. Berrios (2007), Study of the coastal low cloud in the northern coast of Chile: Variability and tendency, paper presented at 4th International Conference on Fog, Fog Collection and Dew, La Serena, Chile, 22–27 July.

Rasmusson, E., and T. Carpenter (1982), Variations in tropical sea surface temperature and surface wind fields associated with the Southern Oscillation/El Niño, *Mon. Weather Rev.*, *110*, 354–384.

Rossow, W., and R. Schiffer (1999), Advances in understanding clouds from ISCCP, *Bull. Am. Meteorol. Soc.*, *80*, 2261–2287.

Rundel, P. W., P. Villagra, M. Dillon, S. Roig-Juñent, and G. Debandi (2007), Arid and semi-arid ecosystems, in *The Physical Geography of South America*, edited by T. T. Veblen et al., pp. 158–183, Oxford Univ. Press, New York.

Rutllant, J. A., H. Fuenzalida, and P. Aceituno (2003), Climate dynamics along the arid northern coast of Chile: The 1997–1998 Dinámica del Clima de la Región de Antofagasta (DICLIMA) experiment, *J. Geophys. Res.*, *108*(D17), 4538, doi:10.1029/2002JD003357.

Schemenauer, R. S., P. Cereceda, and H. Fuenzalida (1988), A neglected water resource: The Camanchaca of South America, *Bull. Am. Meteorol. Soc.*, *69*, 138–147.

Schubert, W., J. Wakefield, E. Steiner, and S. K. Cox (1979), Marine stratocumulus convection. Part I: Governing equations and horizontally homogeneous solutions, *J. Atmos. Sci.*, *36*, 1286–1307.

Shaffer, G., S. Hormazábal, O. Pizarro, and S. Salinas (1999), Seasonal and interannual variability of currents and temperature over the slope off central Chile, *J. Geophys. Res.*, *104*, 29,951–29,961.

Smith, T., and R. Reynolds (2004), Improved extended reconstruction of SST (1854–1997), *J. Clim.*, *17*, 2466–2477.

Squeo, F., Y. Tracol, D. López, J. R. Gutiérrez, A. M. Cordova, and J. R. Ehleringer (2006), ENSO effects on primary productivity in southern Atacama Desert, *Adv. Geosci.*, *6*, 273–277.

Squeo, F. A., G. Arancio, and J. Novoa-Jerez (2004), Heterogeneidad y diversidad Florística del Bosque de Fray Jorge, in *Historia Natural del Parque Nacional Bosque Fray Jorge*, edited by F. A. Squeo, J. R. Gutiérrez, and I. R. Hernández, pp. 173–185, Ediciones Univ. de La Serena, La Serena, Chile.

Thompson, M., B. Palma, J. T. Knowles, and N. M. Holbrook (2003), Multi-annual climate in Parque Nacional Pan de Azúcar, Atacama Desert, *Chile, Rev. Chil. Hist. Nat.*, *76*, 235–254.

Turton, J. D., and S. Nicholls (1987), A study of the diurnal variation of stratocumulus using a multiple mixed layer model, *Q. J. R. Meteorol. Soc.*, *113*, 969–1009.

Villagrán, C., and J. J. Armesto (1980), Relaciones florísticas entre las comunidades relictuales del Norte Chico y la Zona Central con el bosque del Sur de Chile, *Bol., Mus. Nac. Hist. Nat.*, *37*, 85–99.

Villagrán, C., J. J. Armesto, F. Hinojosa, J. Cuvertino, C. Pérez, and C. Medina (2004), El enigmático origen del bosque relicto de Fray Jorge, in *Historia Natural del Parque Nacional Bosque Fray Jorge*, edited by F. A. Squeo, J. R. Gutiérrez, and I. R. Hernández, pp. 173–185, Ediciones Univ. de La Serena, La Serena, Chile.

Vogelmann, H. W. (1973), Fog precipitation in the cloud forests of eastern Mexico, *Biogeoscience*, *23*, 96–100.

Wood, R., and C. S. Bretherton (2004), Boundary layer depth, entrainment, and decoupling in the cloud-capped subtropical and tropical marine boundary layer, *J. Clim.*, *17*, 3576–3588.

Yulaeva, E., and J. M. Wallace (1994), The signature of ENSO in global temperature and precipitation fields derived from the microwave sounding unit, *J. Clim.*, *7*, 1719–1736.

J. Barichivich and D. A. Christie, Laboratorio de Dendrocronología, Facultad de Ciencias Forestales, Universidad Austral de Chile, Valdivia Casilla 567, Chile.

R. Garreaud, Department of Geophysics, Universidad de Chile, Blanco Encalada 2002, Santiago, Chile. (rgarreau@dgf.uchile.cl)

A. Maldonado, Laboratorio de Paleoambientes, Centro de Estudios Avanzados en Zonas Aridas, Universidad de La Serena, Benavente 980, La Serena, Chile.